Hindawi Publishing Corporation
Journal of Spectroscopy
Volume 2014, Article ID 467185, 6 pages
http://dx.doi.org/10.1155/2014/467185

Research Article

Structural Characterization of Carbon Nanomaterial Film *In Situ* Synthesized on Various Bulk Metals

J. Y. Xu, R. Yang, Z. Z. Fan, and X. C. Lei

College of Materials Science and Engineering, Chongqing University, Chongqing 400030, China

Correspondence should be addressed to J. Y. Xu; junyaoxu@cqu.edu.cn

Received 7 May 2014; Accepted 28 May 2014; Published 19 June 2014

Academic Editor: Wen Zeng

Carbon nanofiber films were prepared via a simple chemical vapor deposition (CVD) method on various bulk metal substrates including bulk 316 L stainless steel, pure cobalt, and pure nickel treated by surface mechanical attrition treatment (SMAT). The microstructures of the carbon nanomaterial film were studied by SEM, TEM, XRD, and Raman spectroscopy. In this paper, bulk metallic materials treated by SMAT served as substrates as well as catalysts for carbon nanomaterial film formation. The results indicate that the carbon nanofiber films are formed concerning the catalytic effects of the refined metallic particles during CVD on the surface of SMAT-treated bulk metal substrates. However, distinguished morphologies of carbon nanomaterial film are displayed in the case of the diverse bulk metal substrates.

1. Introduction

Surface mechanical attrition treatment (SMAT) is proved to be an effective technique to achieve nanocrystallization in the surface layer of the bulk materials by means of severe plastic deformation (SPD). It has been successfully applied in a variety of materials including pure metals, alloys, and steels [1, 2]. With this kind of surface modification, the surface properties, for example, diffusivities, can be greatly enhanced [3–5]. Carbon nanomaterials, on the other hand, have attracted much attention due to their excellent properties and the inspiring applications [6]. Carbon nanomaterial film with rational structural design synthesized directly on the surface of bulk substrate displays wide potential applications [7, 8]. Thus, various templates or new techniques are developed [9–11]. However, few of them are facile and of low cost. Recently, using hybrid SMAT, that is, SMAT followed by chemical vapor deposition (CVD), carbon nanomaterials have been successfully synthesized *in situ* on the surface of bulk transition metals [12, 13]. It is a new way to obtain functional carbon nanomaterial film *in situ* on bulk metals, which shows many prospective potential applications.

To get more details about the synthesized carbon products, in current work, scanning electron microscopy (SEM), transmission electron microscopy (TEM), X-ray diffraction (XRD), and Raman spectroscopy were used to characterize the resulting carbon nanomaterials.

2. Experimental Details

Three metallic plates including stainless steel (AISI 316 L), pure cobalt (purity 99.9%), and pure nickel (purity 99.9%) were chosen as substrates to *in situ* synthesize carbon nanomaterial films by method of SMAT followed by CVD. The size of plates was 20 mm in diameter and 1 mm in thickness.

Surface modification was firstly applied on the bulk metallic samples by the SMAT process to achieve nanostructured surface layer. The details of the SMAT were described in the literature [2]. Figure 1 displays the schematic illustration of the SMAT setup. Due to the severe plastic deformation introduced on the sample surface by numerous repeated multidirectional impacts, the metallic grains in the surface were refined into the nanometer regime. The key operation parameters of the SMAT process were outlined as the following: the vibration frequency of the ultrasonic system was 20 kHz, the shot diameter was 2 mm, and the perpetual treatment time was 30 min.

Subsequently, a one-step CVD process was adopted for the synthesis of the nanostructured carbon films. The SMAT samples were inserted into the center of a quartz tube furnace,

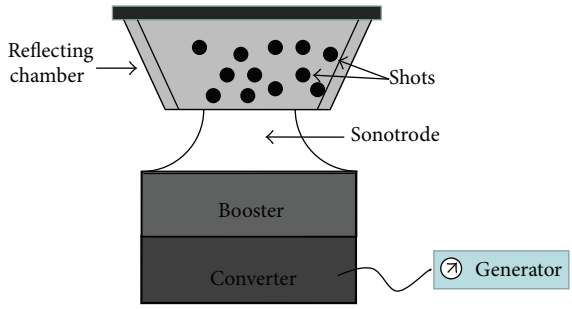

Figure 1: Schematic illustration of the experimental SMAT setup.

which was heated to 550°C. A mixture of $C_2H_2/H_2/N_2$ (50/100/300, v/v/v) was introduced into the tube at a flow rate of 450 sccm (mL/min) and kept for 30 min. After that, the samples were cooled down to room temperature in the furnace with the protection of N_2 atmosphere to obtain the final products.

For the microstructural analysis of carbon nanomaterial films, SEM was carried out on a Sirion, FEI working at 3 kV accelerated voltage. TEM observations were performed using a Philips CM30 microscope working under 300 kV accelerated voltage. XRD analysis was carried out with Cu Kα radiation. Scans were performed at a rate of 0.05°/s, in the range of 2θ = 20–85°. Raman scattering measurements were performed with Jobin Yvon Horiba HR 800 micro-Raman system. Scans were in the range 1000–2000 cm^{-1}, 10 s, 3 to 5 acquisitions per point, using an Ar^+ laser with wavelength of 488 nm.

3. Results and Discussions

After CVD process, black thin films have been obviously formed on the surface of the SMAT areas. SEM and TEM characterizations were performed to estimate the nature of the products and to get more detailed information of the morphology. The films were carefully scratched from the substrates and were dispersed in distilled water using ultrasonication to prepare the specimens for TEM observations. The representative SEM and TEM images of the samples were shown in Figure 2. As can be seen from Figure 2(a), a mixture composed of amorphous carbon, carbon nanofibers, and metallic particles was synthesized on SMAT 316 L stainless steel substrate. Many metallic particles embedded in amorphous carbon are observed (Figure 2(b)). In contrast, residual metal particles are rarely observed on the surface of SMAT Co, and the film mainly composed of carbon nanofibers is formed, as shown in Figures 2(c) and 2(d). The nanofibers have a relatively uniform diameter of about 25 nm despite several much thicker fibers. Most of the carbon nanofibers are curly and entangled with each other. Some metal particles are maintained at the top ends of the fibers, as can be seen from Figure 2(d), which implies that the growth of the carbon nanofibers on SMAT Co might follow the "deposition-diffusion-nucleation-growth" mechanism. Differing from the morphologies of carbon films on SMAT 316 L stainless and SMAT Co, a thick black film composed of carbon products with the appearance as dust clusters was formed on SMAT Ni. Figures 2(e) and 2(f) show the typical SEM and TEM images of the carbon nanomaterials synthesized on SMAT Ni, indicating long and straight thick fibers with a diameter of over 100 nm. Also, there are relatively thin curly fibers around the straight thick fibers.

The phase composition of SMAT metals after CVD process was studied by XRD. Figure 3 collects the XRD data of the obtained products. For the SMAT 316 L stainless steel (Figure 3(a)), it is observed that the XRD patterns contain the diffraction peaks of both the γ austenite phase and the α' martensite phase, indicating that a martensite transformation has taken place during the SMAT process and led to a mixed structure of martensite and austenite. The noncrystal broad peak reveals the presence of the amorphous carbon. The diffraction peak at 2θ = (about 26°) can be indexed as the (002) graphite reflection. The intensity of the diffraction peaks relates to the graphitization degree of the carbon nanofibers. Result deduced from the XRD patterns suggests that graphite products have formed on the SMAT 316 L stainless steel. For the SMAT Co, as shown in Figure 3(b), the diffraction peaks of Co are evidently broadened due to the grain refinement. No obvious noncrystal broad peak is observed, indicating that there is hardly amorphous carbon among the products. The representative peak of graphite C (002) is sharp and smooth, which represents the high degree of long-range order of the carbon products. XRD patterns shown in Figure 3(c) display the peaks of Ni and carbon nanofibers. The representative peak of graphite C (002) (2θ = 26°) is smooth but broader than that of the carbon nanofibers synthesized on SMAT Co, indicating a lower degree of long-range order of the carbon products. Nevertheless, no obvious noncrystal broad peak representing the amorphous carbon is observed. The broadening peaks of Ni may be attributed to nanocrystallization of the metallic surface layer.

Although using the SEM and TEM can directly observe the microstructure of the carbon nanomaterial, the comprehensive graphitization quality cannot be represented. Raman spectroscopy is one of the most valuable techniques for characterizing the deposited carbon by providing the information about the surface molecular vibration [14]. The carbon bond nature of the deposited carbon products over SMAT 316 L stainless steel, Co, and Ni was characterized by Raman spectroscopy and the obtained results are presented in Figure 4. As shown in Figure 4(a), the products synthesized on SMAT 316 L stainless steel exhibit two distinct Raman bands located at around 1359 cm^{-1} and at around 1597 cm^{-1}. The peak at 1597 cm^{-1} is the graphite band (G-band), which implies the high degree of symmetry and order of carbon materials, generally used to identify well-ordered carbon, while the peak at 1359 cm^{-1} is the disorder-induced phonon mode (D-band), which is attributed either to structural imperfection of graphite or to the presence of nanoparticles as well as to the in-plane carbon-carbon stretching vibrations arising. Its shifts and line-width variations are indications of the defects of the crystal lattice. The ratio of the G-band to the D-band represents the amount of sp^2(graphite) clusters in the sample. High G/D ratio represents high graphitization quality.

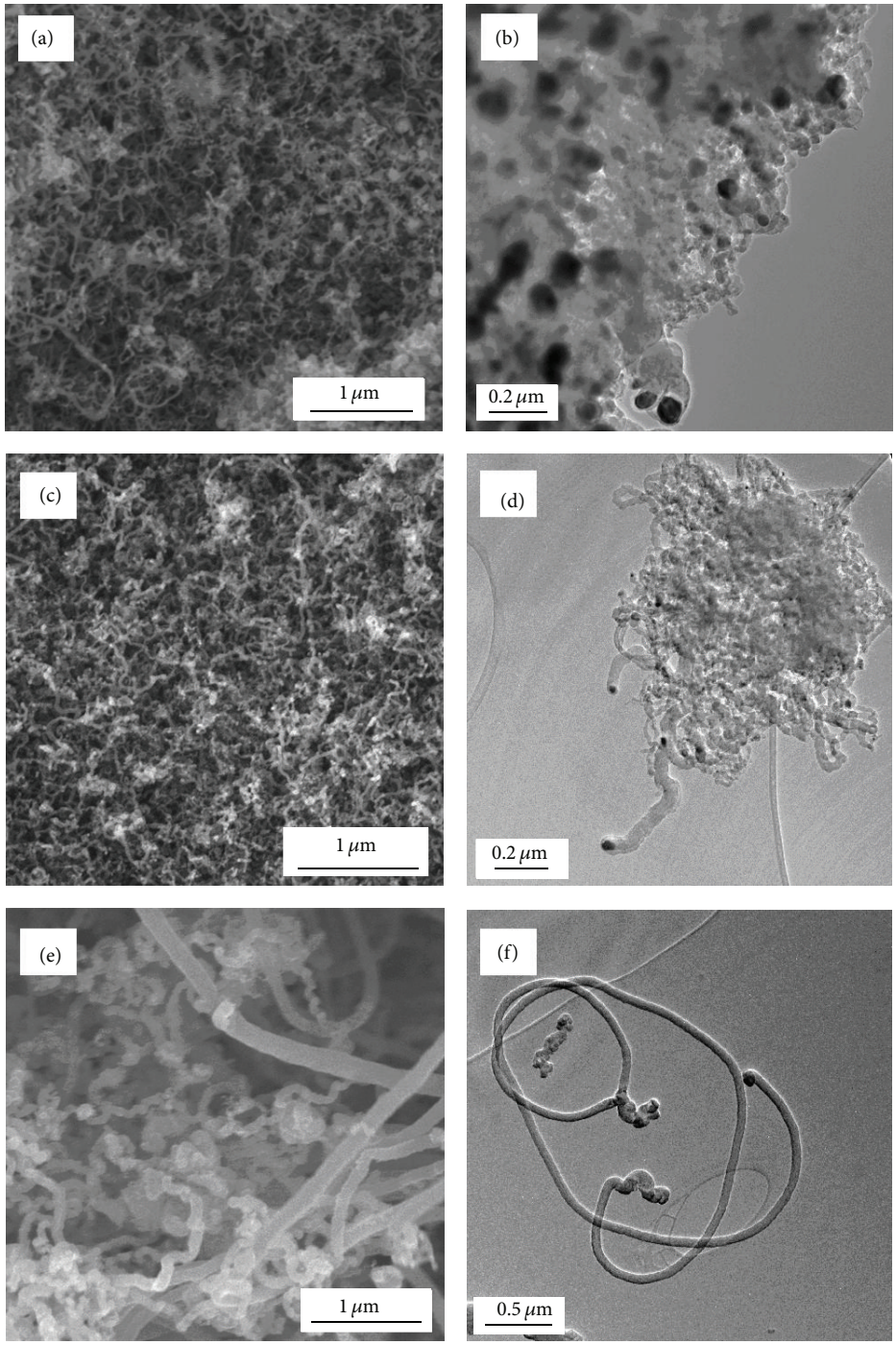

Figure 2: SEM (a, c, and e) and TEM (b, d, and f) images of the carbon nanofibers synthesized on different SMAT metals: (a, b) on SMAT 316 L stainless steel; (c, d) on SMAT Co; and (e, f) on SMAT Ni.

In Figure 4(a), the intensity of peak D is a little lower than that of peak G, which indicates that the products over SMAT 316 L stainless steel have relatively higher graphitization. The products formed on SMAT Co were also characterized by Raman spectroscopy, as shown in Figure 4(b). The figure displays two distinct bands located at 1394 cm^{-1} (D peak) and 1590 cm^{-1} (G peak). Peak G corresponds to sp^2 bonding (due to the graphitic structure) and peak D corresponds to sp^3 bonding (due to the disordered structure in carbon). In this case, the intensity of peak G is much higher than that of peak D, which indicates the carbon with high graphitization. Figure 4(c) displays the Raman spectrum of the carbon nanofibers formed on SMAT Ni, showing two peaks assigned to carbon located at 1342 cm^{-1} (D-band peak) and 1578 cm^{-1} (G-band peak). It is noted that in this case the intensity of D-band peak is comparative with that of G-band peak.

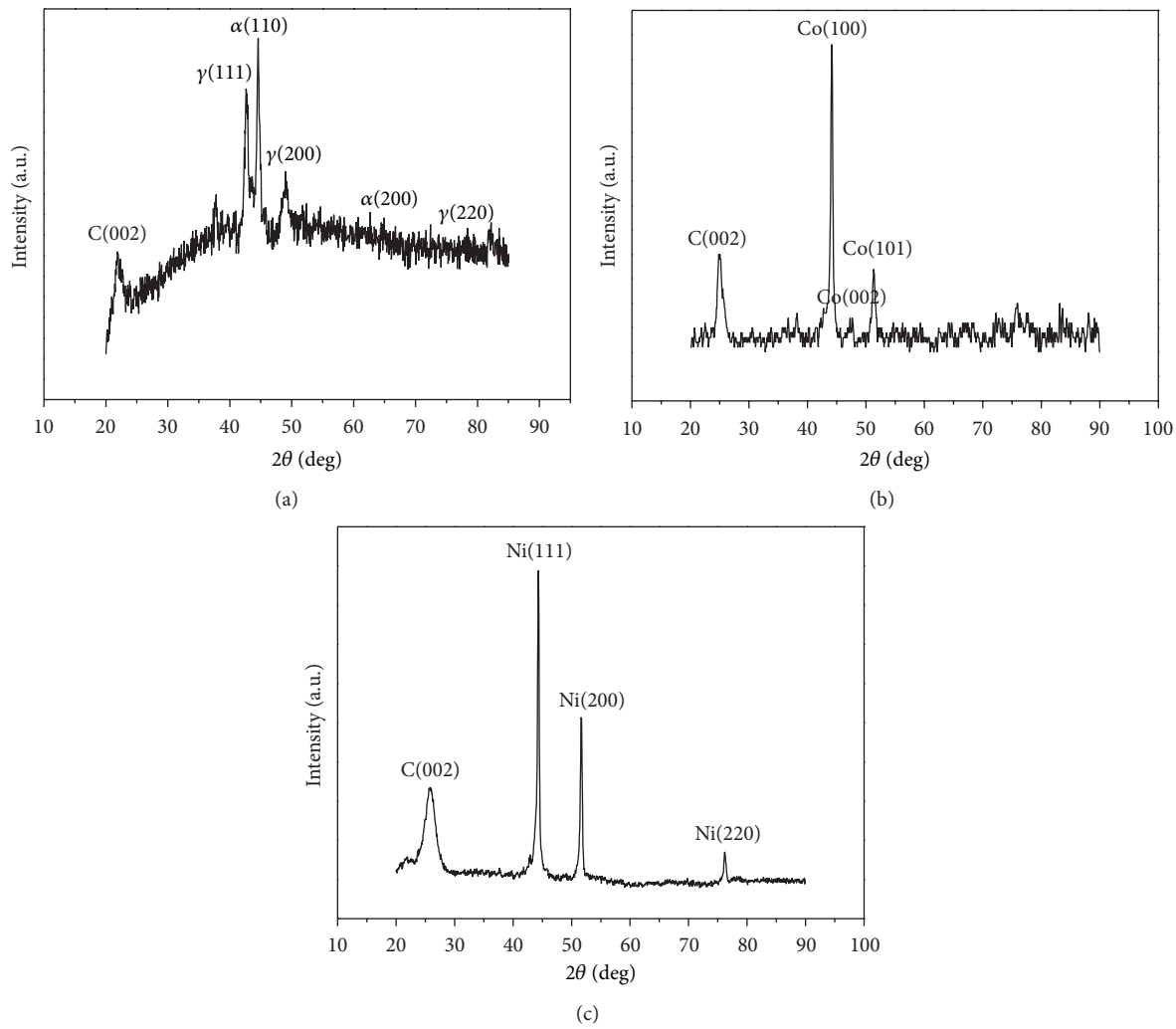

Figure 3: XRD patterns of carbon nanofibers synthesized on (a) SMAT 316 L stainless steel, (b) SMAT Co, and (c) SMAT Ni.

This indicates that two-dimensional disorders existed in the basal plane, which is quite common in pyrolytic carbon materials synthesized by CVD. The existence of a carbon sheet turbostratic structure in the carbon nanomaterial can also result in a significant D-band peak.

The catalytic ability of the transition metals to prepare carbon nanomaterial is thought to be related to the complicated factors including their catalytic activity for the decomposition of volatile carbon compounds, the formation of metastable carbides, and the diffusion of carbon through the metal particles [15]. It was reported in the literatures [16, 17] that the high chemical reactivity of the nanocrystallined metal particles (because of numerous grain boundaries) and a large excess energy in form of nonequilibrium defects bring an extra driving force stored in the SMAT metals. The high concentration of the nonequilibrium defects (dislocations and subgrain boundaries) that are induced by plastic deformation may decrease the activation energy of diffusion and act as fast atomic transfer channels as well.

4. Conclusions

In summary, carbon material films were synthesized on the surface of the SMAT 316 L stainless steel, SMAT Co, and SMAT Ni by means of CVD process. Bulk metallic materials by SMAT surface modification served as substrates as well as catalysts for carbon nanomaterial film formation. Different metallic materials result in carbon nanomaterial film with various morphologies. Carbon nanofibers synthesized on SMAT 316 L stainless steel are not uniform or dense, along with amorphous carbon and many embedded inactive metallic particles. SMAT Co results in rather thin, uniform, and curly carbon nanofibers. These two kinds of carbon nanofibers show significant G-band peak in Raman characterizations, indicating high graphitization in the samples while carbon nanofibers formed on SMAT Ni are straighter, longer, and thicker, showing significant D-band peak in Raman characterization.

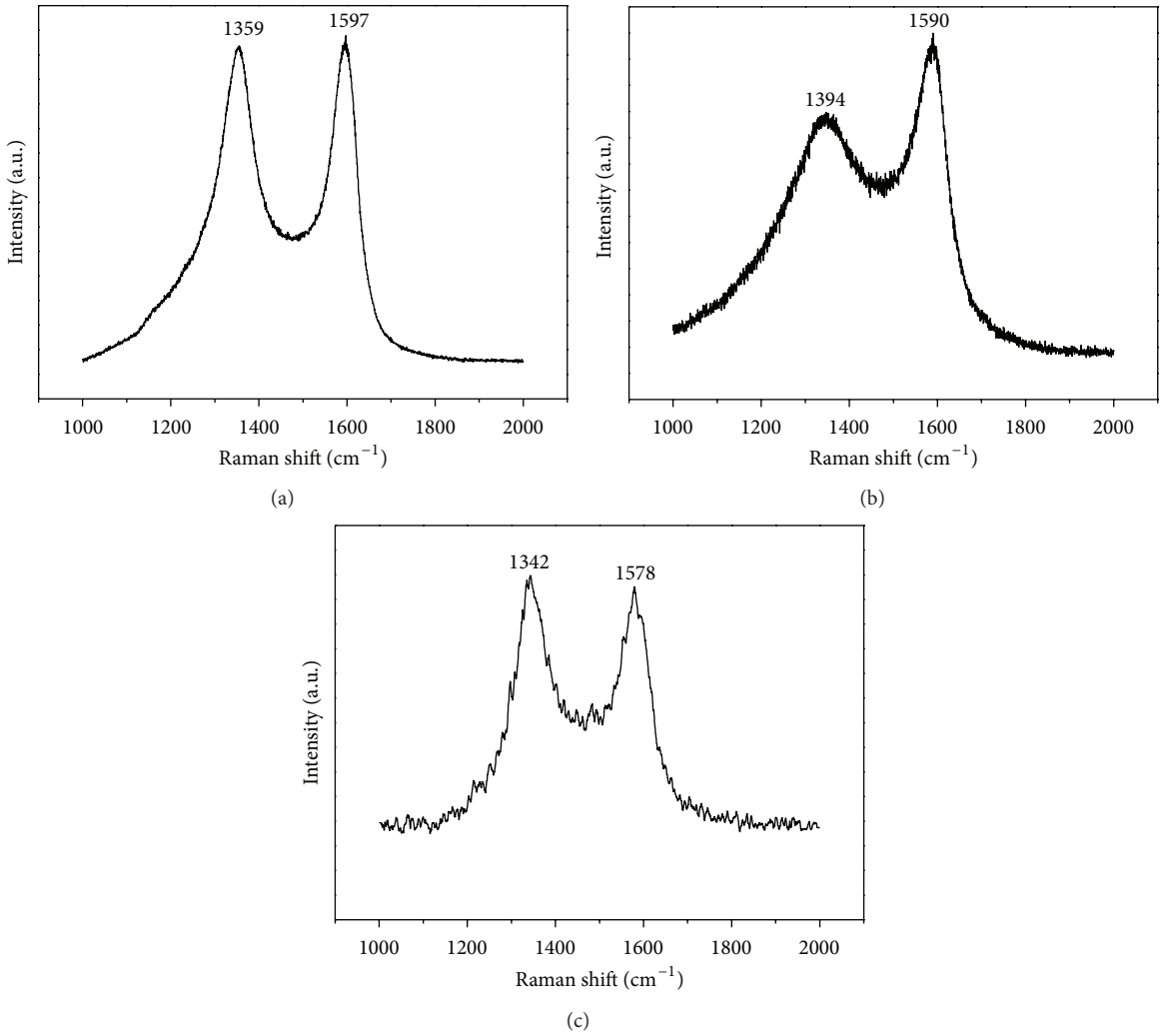

Figure 4: Raman spectrum of carbon nanofibers synthesized on (a) SMAT 316 L stainless steel, (b) SMAT Co, and (c) SMAT Ni.

Conflict of Interests

The authors declare that there is no conflict of interests regarding the publication of this paper.

Acknowledgments

This work was supported by the National Natural Science Foundation of China (Grant no. 51201190), Natural Science Foundation of Chongqing, China (CSTC 2011BB4080), and Fundamental Research Funds for the Central Universities (no. CDJZR12130043).

References

[1] K. Lu and J. Lu, "Surface nanocrystallization (SNC) of metallic materials-presentation of the concept behind a new approach," *Journal of Materials Science and Technology*, vol. 15, no. 3, pp. 193–197, 1999.

[2] K. Lu and J. Lu, "Nanostructured surface layer on metallic materials induced by surface mechanical attrition treatment," *Materials Science and Engineering A*, vol. 375–377, no. 1-2, pp. 38–45, 2004.

[3] W. P. Tong, N. R. Tao, Z. B. Wang, J. Lu, and K. Lu, "Nitriding iron at lower temperatures," *Science*, vol. 299, no. 5607, pp. 686–688, 2003.

[4] Z. B. Wang, K. Lu, G. Wilde, and S. V. Divinski, "Interfacial diffusion in Cu with a gradient nanostructured surface layer," *Acta Materialia*, vol. 58, no. 7, pp. 2376–2386, 2010.

[5] X. Si, B. N. Lu, and Z. B. Wang, "Aluminizing low carbon steel at lower temperatures," *Journal of Materials Science and Technology*, vol. 25, no. 4, pp. 433–436, 2009.

[6] Y. Gogotsi and V. Presser, Eds., *Carbon Nanomaterials*, CRC Press, 2013.

[7] H. C. Chang, C. C. Li, S. F. Jen et al., "All-carbon field emission device by direct synthesis of graphene and carbon nanotube," *Diamond and Related Materials*, vol. 31, pp. 42–46, 2013.

[8] S. Claramunt, O. Monereo, M. Boix et al., "Flexible gas sensor array with an embedded heater based on metal decorated carbon nanofibres," *Sensors and Actuators B: Chemical*, vol. 187, pp. 401–406, 2013.

[9] S. S. Fan, M. G. Chapline, N. R. Franklin, T. W. Tombler, A. M. Cassell, and H. J. Dai, "Self-oriented regular arrays of carbon

nanotubes and their field emission properties," *Science*, vol. 283, no. 5401, pp. 512–514, 1999.

[10] C. Bower, W. Zhu, S. H. Jin, and O. Zhou, "Plasma-induced alignment of carbon nanotubes," *Applied Physics Letters*, vol. 77, no. 6, pp. 830–832, 2000.

[11] R. L. Vander Wal and L. J. Hall, "Carbon nanotube synthesis upon stainless steel meshes," *Carbon*, vol. 41, no. 4, pp. 659–672, 2003.

[12] X. F. Yang and J. Lu, "A new way to synthesize carbon nanofiber film on bulk titanium via hybrid surface mechanical attrition treatment," *Applied Surface Science*, vol. 264, pp. 191–196, 2013.

[13] J. Y. Xu, X. C. Lei, R. Yang, and Z. Z. Fan, "In situ formation of carbon nanomaterials on bulk metallic materials," *Journal of Nanomaterials*, vol. 2014, Article ID 690630, 9 pages, 2014.

[14] M. S. Dresselhaus, G. Dresselhaus, R. Saito, and A. Jorio, "Raman spectroscopy of carbon nanotubes," *Physics Reports*, vol. 409, no. 2, pp. 47–99, 2005.

[15] S. B. Sinnott, R. Andrews, D. Qian et al., "Model of carbon nanotube growth through chemical vapor deposition," *Chemical Physics Letters*, vol. 315, no. 1-2, pp. 25–30, 1999.

[16] Z. B. Wang, N. R. Tao, W. P. Tong, J. Lu, and K. Lu, "Diffusion of chromium in nanocrystalline iron produced by means of surface mechanical attrition treatment," *Acta Materialia*, vol. 51, no. 14, pp. 4319–4329, 2003.

[17] Z. B. Wang, J. Lu, and K. Lu, "Chromizing behaviors of a low carbon steel processed by means of surface mechanical attrition treatment," *Acta Materialia*, vol. 53, no. 7, pp. 2081–2089, 2005.